

This work was written as part of one of the author's official duties as an Employee of the United States Government and is therefore a work of the United States Government. In accordance with 17 U.S.C. 105, no copyright protection is available for such works under U.S. Law.

Public Domain Mark 1.0

<https://creativecommons.org/publicdomain/mark/1.0/>

Access to this work was provided by the University of Maryland, Baltimore County (UMBC) ScholarWorks@UMBC digital repository on the Maryland Shared Open Access (MD-SOAR) platform.

**Please provide feedback**

Please support the ScholarWorks@UMBC repository by emailing [scholarworks-group@umbc.edu](mailto:scholarworks-group@umbc.edu) and telling us what having access to this work means to you and why it's important to you. Thank you.



# Quantum Efficiency Study and Reflectivity Enhancement of Au/Bi Absorbers

R. Hummatov<sup>1,2</sup> · J. S. Adams<sup>1,2</sup> · S. R. Bandler<sup>1</sup> · A. Barlis<sup>1</sup> · S. Beaumont<sup>1,2</sup> · M. P. Chang<sup>1,3</sup> · J. A. Chervenak<sup>1</sup> · A. M. Datesman<sup>1,3</sup> · M. E. Eckart<sup>4</sup> · F. M. Finkbeiner<sup>1,5</sup> · J. Y. Ha<sup>1,6</sup> · R. L. Kelley<sup>1</sup> · C. A. Kilbourne<sup>1</sup> · A. R. Miniussi<sup>1,2</sup> · F. S. Porter<sup>1</sup> · J. E. Sadleir<sup>1</sup> · K. Sakai<sup>1,2</sup> · S. J. Smith<sup>1,2</sup> · N. Wakeham<sup>1,2</sup> · E. J. Wassell<sup>1,3</sup> · E. J. Wollack<sup>1</sup>

Received: 15 August 2019 / Accepted: 21 February 2020 / Published online: 7 March 2020  
© Springer Science+Business Media, LLC, part of Springer Nature 2020

## Abstract

X-ray absorbers of the X-ray Integral Field Unit (X-IFU) microcalorimeters are required to provide high quantum efficiency (QE) for incident X-rays and high reflectivity to longer wavelength radiation. The thickness of the electroplated Au and Bi layers of the absorber is tuned to provide the desired pixel heat capacity and the QE. To calculate the QE precisely, in addition to filling factor, we have included the effects of surface roughness, edge profile of the absorbers and the effects of the different angles of incidence of the incoming X-rays from the X-IFU optic. Based on this analysis, it is found that thickness of the Bi layer needs to be adjusted by 4.3% to achieve the X-IFU QE requirements. To enhance the absorber's rejection of low-energy radiation, a second thin layer of Au is sputter-deposited on top of the Bi layer. Optical measurements in the wavelength range 0.3–20  $\mu\text{m}$  show a significant increase in reflectivity compared to a bare Bi layer.

**Keywords** Transition edge sensor · Microcalorimeter · Au/Bi · Quantum efficiency · Reflectance

---

✉ R. Hummatov  
ruslan.hummatov@nasa.gov

<sup>1</sup> NASA Goddard Space Flight Center, Greenbelt, MD 20771, USA

<sup>2</sup> CRESSST II - University of Maryland, Baltimore County, MD 21250, USA

<sup>3</sup> Science Systems and Applications, Inc. (SSAI), 10210 Greenbelt Rd, Lanham, MD 20706, USA

<sup>4</sup> Lawrence Livermore National Laboratory, Livermore, CA 94550, USA

<sup>5</sup> Sigma Space Corp., 4600 Forbes Blvd., Lanham, MD 20706, USA

<sup>6</sup> SB Microsystems, 806 Cromwell Park Dr, Glen Burnie, MD 21061, USA

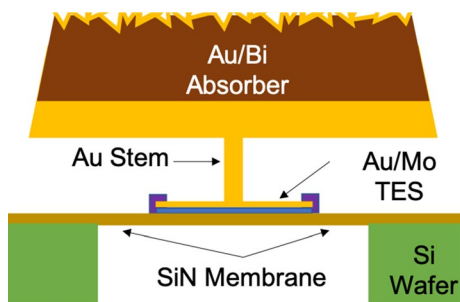
## 1 Introduction

The X-ray Integral Field Unit (X-IFU) is an instrument on the Advanced Telescope for High-ENERgy Astrophysics (ATHENA) space telescope that will use  $\sim 3.2$  kilopixels of transition edge sensor (TES) microcalorimeters [1]. The pixels are being designed to provide full-width-half-maximum (FWHM) instrument energy resolution of  $\Delta E_{\text{FWHM}} = 2.5$  eV at 7 keV. Each microcalorimeter pixel consists of  $\sim 6$ - $\mu\text{m}$ -thick Au/Bi absorber attached to a Mo/Au bilayer sensor with critical temperature around  $T_C \approx 90$  mK as shown in Fig. 1. The absorber is a critical component to the pixel design that not only provides the stopping power for X-rays, or quantum efficiency (QE), but also dominates the total heat capacity budget, which determines the resolution and dynamic range of the pixel, and it also provides reflectivity for longer-wavelength photons, which can be responsible for photon shot noise. In this paper, we report on the design and optimization of the absorbers for X-IFU. In particular, we have studied effects of filling factor, surface roughness and edge profile of the absorbers and the effect of incidence angle of the X-rays on the average quantum efficiency (QE). We also report a new process to increase the reflectivity of the top Bi layer to the low-energy photons (1–20  $\mu\text{m}$  wavelength range) by introducing thin Ti/Au capping layer.

## 2 Absorber Design

To achieve the required instrument energy resolution of  $\Delta E_{\text{FWHM}} = 2.5$  eV up to 7 keV and  $\Delta E_{\text{FWHM}} = 5$  eV at 10 keV, the TES microcalorimeter needs to have a total heat capacity of  $C = 1.1$  pJ/K at  $T_C$ . The heat capacity is chosen as a trade-off between minimizing the intrinsic pixel resolution ( $\Delta E_{\text{FWHM}} \propto \sqrt{C}$ ) at low energies, while also being large enough to ensure the performance is not compromised at the highest energies of interest due to non-linearity. The total heat capacity of the pixel is dominated by the Au layer in the absorber. Both Au and Bi provide high stopping power for X-rays; however, Au is used to provide good lateral thermal conductivity across the absorbers to ensure rapid thermalization at low temperatures (as is needed to avoid any position dependence which degraded the energy resolution performance), while Bi is used to provide additional stopping

**Fig. 1** A diagram of a GSFC TES pixel. Au/Bi absorber is attached to an Au/Mo TES which is suspended by SiN membrane. The absorber has a trapezoidal shape and a rough surface. A thin Au capping layer is added to improve reflectance at 1–20  $\mu\text{m}$  wavelength range (Color figure online)



power without adding significant additional heat capacity (due to its low electron density). The relative thicknesses of Au and Bi layers are tuned to simultaneously obtain the target  $C$  while achieving the required QE. At the same time, the gaps between absorbers must be minimized to achieve high areal filling factor. Our current X-IFU TES microcalorimeters consist of a 2- $\mu\text{m}$  Au layer plus a 3.75- $\mu\text{m}$  Bi bilayer absorber. They have a pixel pitch of 250  $\mu\text{m}$ . The most recent X-IFU array requirements are for pixels with a 275- $\mu\text{m}$  pitch and  $\sim 5\text{-}\mu\text{m}$  gap between pixels.

The Au/Bi bilayer absorber is fabricated in two main steps. First, a continuous layer of absorber material is deposited by pulsed electroplating of Au and Bi layers over the entire array in separate Au and Bi plating baths. Here, electroplating of Au is preferred over other microfabrication processes such as thermal evaporation and sputtering since the films produced have higher residual resistance ratio (RRR), providing better thermalization properties at low temperatures. Second, ion milling is used to isolate individual absorbers [2]. Completed absorbers typically have a rough surface finish due to the formation of a Bi grain structure. They also have a slightly angled edge profile due to the required positioning of the ion milling gun relative to sample. The effects of the surface roughness of the Bi and edge profile of the absorber need to be addressed when determining the QE. Quantitative information about the surface roughness of a typical Bi layers was obtained by using a 3D surface profiler. This measurement was carried out on a sample that was fabricated by using a grain refiner additive to the Bi bath [3]. This recipe is found to produce a Bi layer with fewer voids, less trapped precipitates, slightly higher reflectivity and a visibly smoother surface [4].

Stray power from the radiative heat load from warmer stages of the X-IFU cryostat can cause thermal fluctuations in the detector array. These fluctuations can be sensed in the TES microcalorimeters, causing a shot noise that can degrade the performance. To prevent this, optical blocking filters at various temperature stages of the cryostat are being developed for X-IFU [5]. In order to minimize the requirements of the infrared blocking filters and potentially improve the overall filter throughput at low energies, it is desirable for the Au/Bi absorbers to have as high a reflectivity as possible. In a new process, we are experimenting with depositing thin layers of Au with a Ti adhesion layer on top of the main absorber layers to increase the reflectivity. This thin top layer is using an e-beam evaporator with a planetary rotation system that ensures evaporations at a variety of angles in an attempt to coat the rough surface as continuously as possible.

## 2.1 Quantum Efficiency Study

The total QE requirements for X-IFU are currently 96, 87 and 63% at 1, 7 and 9.5 keV, respectively. This includes both the vertical QE and the areal filling factor. Since these numbers are close to technically achievable limits, the QE needs to be calculated precisely. The vertical QE of Au/Bi absorber is calculated using the Lambert–Beer law for attenuation of X-rays in these two materials:

$$QE = 100\% * \left( 1 - \exp \left( -\frac{t_{Bi}}{\mu_{Bi}} \right) \exp \left( -\frac{t_{Au}}{\mu_{Au}} \right) \right) \quad (1)$$

Here,  $t_{Bi}$  and  $t_{Au}$  are the thicknesses of the Bi and Au layers and  $\mu_{Bi}$  and  $\mu_{Au}$  are the corresponding X-ray attenuation lengths for different X-ray energies [6]. The X-rays interact with the absorbers predominantly through the photoelectric effect in the energy range of interest. Therefore, their energy is either completely absorbed or not changed as they propagate through the absorber material. Considering only the vertical QE, the optimal thicknesses to achieve 1.1 pJ/K at 90 mK and 90% QE at 7 keV would require 2  $\mu\text{m}$  Au and 3.75  $\mu\text{m}$  Bi. Here, the heat capacity includes the heat capacities of the Au/Bi absorber (85% + 2%), Mo/Au bilayer TES sensor (8%) and the SiN membrane (5%) [7, 8]. If we consider a microcalorimeter array with 98% filling factor and with perfectly vertical absorber edges, the total QE would decrease to 88.2%. This estimation can be further refined to include the effects of the surface roughness and absorber edge profile.

The surface of a 3.44- $\mu\text{m}$ -thick bismuth layer of the type fabricated for our absorbers was electroplated onto a Ti/Au seed layer to enable us to study its surface profile using a 3D optical interference profiler. A scanning electron microscope (SEM) image and 3D model of this surface are shown in Fig. 2 (left top and bottom). A histogram of the surface heights was produced from an average of ten measurements at various sites on the surface. The shape of this histogram can be fit by a Gaussian distribution with a 0.6- $\mu\text{m}$  standard deviation. The grain size of the Bi is expected to be proportional to the thickness of the deposited layer [9]. Thus, by scaling and adding this variation to 3.75- $\mu\text{m}$  Bi and 2- $\mu\text{m}$  smooth Au layer, we can determine a histogram of the heights within a single Au/Bi absorber as shown in Fig. 2 (right). We use the thickness values from this histogram with Eq. 1, to

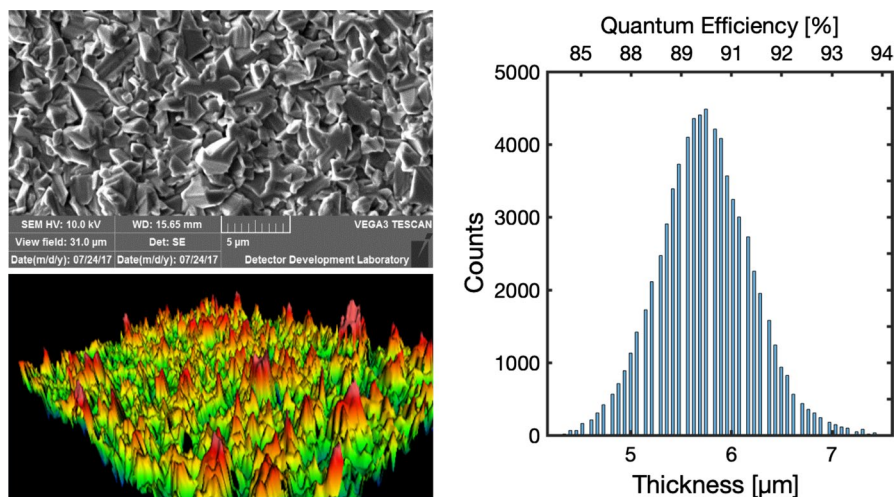


**Fig. 2** (Left top) SEM image of the electroplated Bi surface. (Left bottom) Surface roughness of the Bi surface seen by surface interferometer. (Right) Corresponding histogram of the surface roughness of Au/Bi absorbers. The bottom axis is the thickness, and the top axis is the inferred QE (Color figure online)

determine the corresponding QEs, which are labeled on the top axis of the histogram plot. The weighted average of these is 90.11%, which is 0.13% decrease from QE of 90.24% for absorber without the roughness.

An optical microscope was used to obtain the edge profile of the absorbers. To determine the angle of the absorber sidewalls, we measured the distance between two adjacent absorbers at the top of the absorbers and at the bottom of the absorbers by focusing to the top and bottom surfaces and determining the height from the difference between the top and bottom focus. The gaps were measured to be  $\sim 10\ \mu\text{m}$  at the top and  $\sim 6\ \mu\text{m}$  at the bottom. Here, the top gap is set by the design of the photoresist mask, and the bottom gap is set by the ion mill angle. If smaller gaps are desired to increase the fill factor, there will generally be an increased chance of producing shorts in between absorbers from Bi grains that are not perfectly milled away, and thus, the yield will be reduced.

In Fig. 3 (left), the QE of an Au/Bi absorber with trapezoidal profile is plotted for fixed top gaps and for various bottom gaps, at energies of 7 (left y-axis) and 9.5 keV (right y-axis). The X-IFU QE requirements are plotted as dotted horizontal lines according to their respective axes. Currently, our typical laboratory absorbers have a  $\sim 10\text{-}\mu\text{m}$  top gap and  $\sim 6\text{-}\mu\text{m}$  bottom gap, and the QEs are denoted by the red circles, which are below the requirements at both energies. To reach the requirements, the next iteration of Au/Bi absorbers is being developed with reduced gap widths, and  $\sim 7\text{-}\mu\text{m}$  top and  $\sim 4\text{-}\mu\text{m}$  bottom gap has already been achieved, pushing the QEs to the green circles.

We have also looked at whether there is any potential effect on the QE from the range of angles from the incoming X-rays, leading to slightly increased path lengths

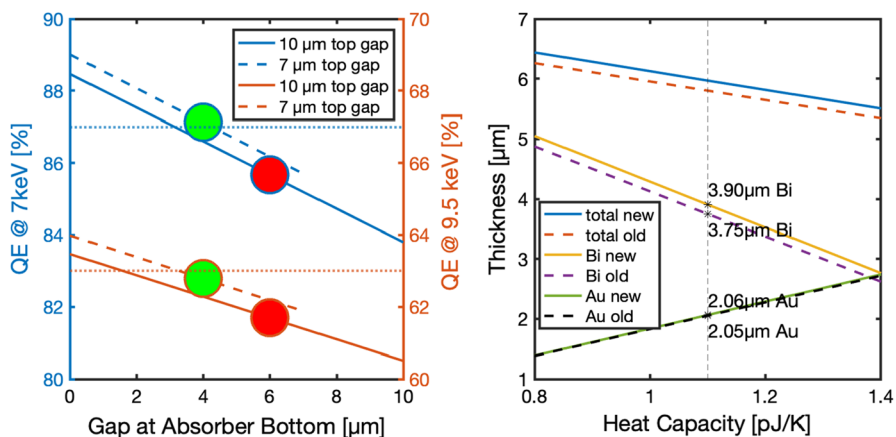


**Fig. 3** (Left) QE of trapezoidal Au/Bi absorber at 7 and 9.5 keV. The requirements are 87% and 63%, respectively, shown as dotted horizontal lines. Thickness ( $2 + 3.75\ \mu\text{m}$ ) and top gaps (7  $\mu\text{m}$  and 10  $\mu\text{m}$ ) of the absorbers are fixed, and the bottom gaps are varied between 0 and 10  $\mu\text{m}$ . Red and green circles show estimated QEs with 4  $\mu\text{m}$  and 6  $\mu\text{m}$  bottom gaps with  $\pm 0.5\ \mu\text{m}$  uncertainty. (Right) Optimal thicknesses to achieve 0.8–1.4 pJ/K target heat capacities while providing 63% QE at 9.5 keV. Dashed lines are obtained by taking into account only the filling factor, while solid lines are obtained by additionally including surface roughness and edge profile with fixed 10  $\mu\text{m}$  top gap and 5.5  $\mu\text{m}$  bottom gap. The vertical dashed line at 1.1 pJ/K is the target heat capacity (Color figure online)

for the X-rays in the absorber material. ATHENA's telescope will have a 12-m focal length, and the X-ray optic has a 3-m diameter. The X-rays will be focused by using silicon pore optics [10]. Thus, the incident angle varies between  $1^\circ$  and  $7^\circ$ . By using a typical effective area versus incident angle data set for this type of optic, we calculated a weighted averaging for the change in QE at 7 keV and found that this effect would be less than 0.01% at this energy. At lower energies, the QE approaches unity at this thickness scale, and at higher energies, there is very little effective area of the optic, so 7 keV is the energy at which the effect of a varying incident angle has the potential to be the greatest.

By considering the fill factor, surface roughness and the edge profile in our QE calculation, we calculated the target thicknesses of the Au and Bi layers for pixels which have a range of heat capacities between 0.8 and 1.4 pJ/K, as shown in Fig. 3 (right). The layer thicknesses have been chosen to achieve 63% QE for 9.5 keV X-rays, since this requirement needs more thickness than the other energies. Based upon these calculations and depending on the required heat capacity, we need to increase the Bi thickness over the current thickness only by approximately 4.3% and Au thickness by only 0.5% over our current design thicknesses. Both of these changes are not significant and can be easily achieved in fabrication. Therefore, this is a more robust solution for meeting QE requirements than changing the gap size.

### 3 Reflectivity Enhancement

While the X-IFU Au/Bi absorbers are optimized to absorb 0.2–12 keV X-rays, optical and infrared radiation from higher temperature stages of the X-IFU cryostat, which are not detected as a TES signal, produces shot noise that degrades detector performance. To reduce these, infrared blocking filters made of aluminized polyimide are typically located at different temperature stages [5]. Additionally, it is currently required for the X-IFU that the Au/Bi absorbers have more than 40% reflectance in the wavelength range of 1–20  $\mu\text{m}$ . This requirement was based upon the measured reflectance of a number of samples of our electroplated Bi at room temperature. Based upon this assumed reflectance, the IR blocking filters have been designed to meet the required X-ray transmittance, while remaining sufficiently rugged to not risk becoming torn.

To improve the reflectance of the Au/Bi absorbers and ease the requirements on the filters, we have introduced an Au capping layer with a 5-nm Ti adhesion layer. This layer was deposited by using e-beam evaporation, during which the deposition angle was varied to increase the coverage of the holes/grains on the Bi surface. In order to compare the reflectance of bare Bi with Bi that has various Au capping layer thicknesses, the total hemispherical reflectance (THR) was measured using a Bruker IFS 125HR spectrometer at room temperature over a spectral range spanning 0.3–20  $\mu\text{m}$ . The photometric accuracy of the integrating sphere used for these measurements was around 2–3%. Results from these measurements and also the reflectance of bulk Au from the literature [11] are plotted in Fig. 4. The two bare Bi samples were 3.62  $\mu\text{m}$  and 3.44  $\mu\text{m}$  thick and were fabricated using our regular Bi recipe and improved recipe with grain refiner additive, respectively. The



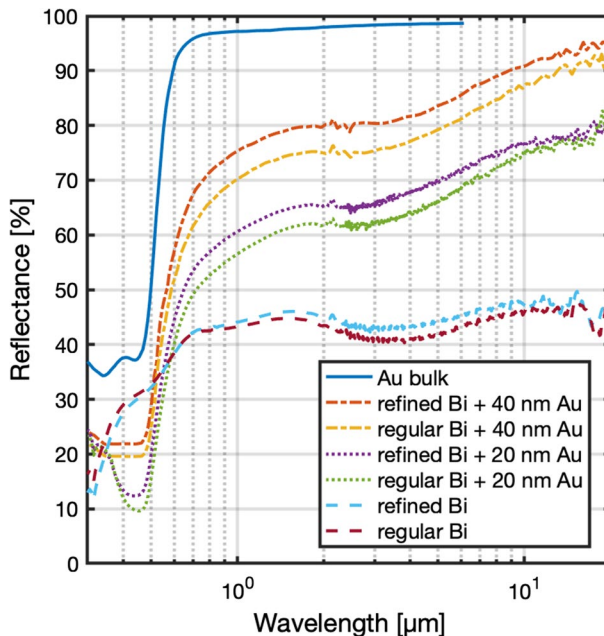


**Fig. 4** THR of electroplated Bi samples. The two bottom dashed lines are from bulk Bi samples that were fabricated by using our regular Bi recipe and recipe with grain refiner additive. Adding 20-nm (dotted lines) and 40-nm (dash-dotted lines) Au capping layer increases the THR in 1–20  $\mu\text{m}$  wavelength range. Reflectance of bulk Au (solid line) from literature [11] is plotted for comparison (Color figure online)

reflectance of these two samples was  $\sim 45\%$  in the 1–20  $\mu\text{m}$  wavelength range with the former being slightly higher. A 20-nm Au capping layer increases the reflectance up to around 60–65%, and a 40-nm capping layer gives around 75–80%. The difference in reflectivity of the two Bi samples is increased as the thickness of the capping layer is increased. For the samples with an Au capping layer, the reflectance starts to increase with increasing wavelength around 3  $\mu\text{m}$ , where the radiation wavelength starts to become comparable with the Bi grain size. The skin depth of Au at 1  $\mu\text{m}$  is about 4.5 nm; thus, a uniform  $\sim 15$ -nm layer of Au is anticipated to approximate the material's bulk reflectance. Therefore, the measured reflectance suggests that Bi is not covered by a continuous layer of sufficiently thick Au, which is probably due to its surface roughness (see SEM image in Fig. 2). Complete coverage could potentially be achieved by increasing the Au thickness. Our e-beam evaporated Au has an RRR of  $\sim 3$ ; thus, we expect at cryogenic temperatures a scattering of the charge carriers in Au will decrease with decreasing temperature, and this could improve the reflectivity of the Au capping layer. On the other hand, RRR of the Bi layer can be less than 1 [2]; thus, at low temperatures, it is expected that the reflectance of our Bi layer can be less than what we have measured at room temperature.

The contribution of the capping layer to the total heat capacity for 20 nm and 40 nm of Au is 1% and 2%, respectively, and to the QE is 0.1% and 0.2%, respectively. To verify that the additional thin top Au layer does not cause any degradation



to the TES microcalorimeter performance, we tested a complete X-ray microcalorimeter with a 20-nm Au capping layer. We measured their spectral performance when irradiated with 5.9 keV and 6.4 keV Mn K X-rays and measured the energy resolution at 5.9 keV to be 2.3 eV FWHM. This spectral performance was consistent with the expected energy resolution based upon the X-ray signal sizes and shapes and also the measured noise spectrum. It was also identical to the performance of some pixels of the identical design, but without the thin gold capping layer. A recent study of the extended line spread function of this type of microcalorimeter by our group did not find any correlation between the absorber design, including Au capping layer, and the extended line spread function [12].

## 4 Conclusions

We have determined the required thicknesses of Au and Bi layers to achieve the desired quantum efficiencies in TES microcalorimeters designed for the ATHENA X-IFU for a range of different required heat capacities. We have included in our estimates the effects of surface roughness, edge profile and the angles of incident X-rays, in addition to the filling factor, in our optimization of the Au and Bi thicknesses. We have also found that the reflectivity of the top Bi in the 0.3–20  $\mu\text{m}$  wavelength range is increased from 45% to up to 80% at room temperature from the addition of 40 nm of an Au capping layer with a 5-nm Ti adhesion layer. This value is expected to increase at the operating temperature of the detectors.

**Acknowledgements** The authors wish to thank NASA's Astrophysics Division for their generous support of this work. Part of this work was performed under the auspices of the U.S. Department of Energy by Lawrence Livermore National Laboratory under Contract DE-AC52-07NA27344.

## References

1. D. Barret et al., Proc. SPIE **9905**, 9905–9983 (2016). <https://doi.org/10.1117/12.2312409>
2. A.-D. Brown et al., J. Low Temp. Phys. **151**, 413 (2008). <https://doi.org/10.1007/s10909-007-9669-2>
3. A.R. Rajamani et al., J. Phys. Chem. C **120**(39), 22398 (2016). <https://doi.org/10.1021/acs.jpcc.6b06924>
4. Presented at ASC 2018 by E. J. Wassell
5. M. Barbera et al., Proc. SPIE **9144**, 91445U (2014). <https://doi.org/10.1117/12.2057403>
6. [https://henke.lbl.gov/optical\\_constants/atten2.html](https://henke.lbl.gov/optical_constants/atten2.html)
7. M.E. Eckart et al., AIP Conf. Proc. **1185**, 430 (2009). <https://doi.org/10.1063/1.3292370>
8. S.J. Smith et al., Proc. SPIE **9905**, 9905–9985 (2016). <https://doi.org/10.1117/12.2231749>
9. L.M. Gades et al., IEEE Trans. Appl. Supercond. **27**(4), 1–5 (2017). <https://doi.org/10.1109/TASC.2017.2662007>
10. M.J. Collon et al., Proc. SPIE **9144**, 91442G (2014). <https://doi.org/10.1117/12.2057347>
11. D. Rakić et al., Appl. Opt. **37**, 5271 (1998). <https://doi.org/10.1364/AO.37.005271>
12. M.E. Eckart et al., IEEE Trans. Appl. Supercond. **29**(5), 1–5 (2019). <https://doi.org/10.1109/TASC.2019.2903420>